2014

Geochronological, morphometric and geochemical constraints on the Pampas Onduladas long basaltic flow (Payún Matrú Volcanic Field, Mendoza, Argentina)

Venera Espanon
University of Wollongong, vre981@uowmail.edu.au

Allan Chivas
University of Wollongong, toschi@uow.edu.au

David Phillips
University of Melbourne, dphillip@unimelb.edu.au

Erin L. Matchan
University of Melbourne

Anthony Dosseto
University of Wollongong, tonyd@uow.edu.au

Publication Details

Espanon, V. R., Chivas, A. R., Phillips, D., Matchan, E. L. & Dosseto, A. (2014). Geochronological, morphometric and geochemical constraints on the Pampas Onduladas long basaltic flow (Payún Matrú Volcanic Field, Mendoza, Argentina). Journal of Volcanology and Geothermal Research, 289 114-129.

Geochronological, morphometric and geochemical constraints on the Pampas Onduladas long basaltic flow (Payún Matrú Volcanic Field, Mendoza, Argentina)

Abstract

The Pampas Onduladas flow in southern Mendoza, Argentina, is one of the four longest Quaternary basaltic flows on Earth. Such flows (> 100 km) are relatively rare on Earth as they require special conditions in order to travel long distances and there are no recent analogues. Favourable conditions include: a gentle topographic slope, an insulation process to preserve the melt at high temperature, and a large volume of lava with relatively low viscosity. This study investigates the rheological and geochemical characteristics of the ~ 170 km long Pampas Onduladas flow, assessing conditions that facilitated its exceptional length. The study also reports the first geochronological results for the Pampas Onduladas flow. 40Ar/39Ar step-heating analyses of groundmass reveal an eruption age of 373 ± 10 ka (2σ), making the Pampas Onduladas flow the oldest Quaternary long flow. The methods used to assess the rheological properties include the application of several GIS tools to a digital elevation model (DEM) to determine the length, width, thickness, volume and topographic slope of the flow as well as algorithms to determine its density, viscosity and temperature. The slope of the Pampas Onduladas flow determined from the initial part of the flow on the eastern side of La Carbonilla Fracture to its end point in the province of La Pampa is 0.84% (0.29°), the steepest substrate amongst long Quaternary flows. The rheological properties, such as density viscosity and temperature from the Pampas Onduladas flow are similar to values reported for other long Quaternary flows. However, the minimum volume calculated is relatively low for its length compared with other long Quaternary flows. Therefore, the extension of the Pampas Onduladas flow was probably controlled by a steep slope, combined with an insulating mechanism, which helped in providing optimal conditions for a travel length of almost 170 km.

Keywords

Pampas Onduladas, Long lava flow, Rheology, Payún Matrú Volcanic Field

Disciplines

Medicine and Health Sciences | Social and Behavioral Sciences

Publication Details

Espanon, V. R., Chivas, A. R., Phillips, D., Matchan, E. L. & Dosseto, A. (2014). Geochronological, morphometric and geochemical constraints on the Pampas Onduladas long basaltic flow (Payún Matrú Volcanic Field, Mendoza, Argentina). Journal of Volcanology and Geothermal Research, 289 114-129.

Geochronological, morphometric and geochemical constraints on the Pampas Onduladas long basaltic flow (Payún Matrú Volcanic field, Mendoza, Argentina)

Venera R. Espanon [a,b*], Allan R. Chivas[a], David Phillips[c], Erin L. Matchan[c] and Anthony Dosseto[a,b]

[a] *GeoQuEST Research Centre*, *School of Earth & Environmental Sciences, University of Wollongong, NSW 2522, Australia.*

[b] *Wollongong Isotope Geochronology Laboratory, School of Earth & Environmental Sciences, University of Wollongong, NSW 2522, Australia.*

[c] *School of Earth Sciences, The University of Melbourne, Parkville, VIC 3010, Australia.*

Allan R. Chivas: toschi@uow.edu.au

David Phillips: dphillip@unimelb.edu.au

Erin L. Matchan: ematchan@unimelb.edu.au

Anthony Dosseto: tony_dosseto@uow.edu.au

*Corresponding author. Tel.: +61 24221 5899; fax: +61 242214250

E-mail address: vre981@uowmail.edu.au

Abstract

The Pampas Onduladas flow in southern Mendoza, Argentina, is one of the four longest Quaternary basaltic flows on Earth. Such flows (>100 km) are relatively rare on Earth as they require special conditions in order to travel long distances and there are no recent analogues. Favourable conditions include: a gentle topographic slope, an insulation process to preserve the melt at high temperature, and a large volume of lava with relatively low viscosity. This study investigates the rheological and geochemical characteristics of the ~170 km long Pampas Onduladas flow, assessing conditions that facilitated its exceptional length. This study also reports the first geochronological results for the Pampas Onduladas flow. $^{40}Ar/^{39}Ar$ step-heating analyses of groundmass reveal an eruption age of 373 ± 10 ka (2σ), making the Pampas Onduladas flow the oldest Quaternary long flow.

The methods used to assess the rheological properties include the application of several GIS tools to a digital elevation model (DEM) to determine the length, width, thickness, volume and topographic slope of the flow as well as algorithms to determine its density, viscosity and temperature. The slope of the Pampas Onduladas flow determined from the initial part of the flow on the eastern side of La Carbonilla fracture to its end point in the province of La Pampa is 0.84% (0.29°), the steepest substrate amongst long Quaternary flows. The rheological properties, such as density viscosity and temperature from the Pampas Onduladas flow are similar to values reported for other long Quaternary flows. However, the minimum volume calculated is relatively low for its length compared with other long Quaternary flows. Therefore, the extension of the Pampas Onduladas flow was probably controlled by a steep slope, combined with an insulating mechanism, which helped in providing optimal conditions for a travel length of almost 170 km.

1 Introduction

Long basaltic flows (>100 km) produced in a single volcanic eruption are unusual on Earth (but common on Mars), as they require relatively large lava volumes and steep slopes (Keszthely and Self, 1998; Keszthely et al., 2004). For the Quaternary (<2.6 Ma), only four flows have been reported to be longer than 100 km, and there are no historic analogues of long flows. The four long Quaternary flows recognised are: the Toomba and Undara flows in Queensland, Australia (Stephenson et al., 1998); the Thjorsa flow in Iceland (Vilmundardottir, 1977); and the Pampas Onduladas flow in Mendoza, Argentina (Pasquarè et al., 2005). These have reported volumes greater than 12 km^3 and a pahoehoe character. Some of the basic requirements for long basaltic flows are: i) an insulating mechanism to maintain the lava at high temperature; and ii) a large volume of erupted lava (Pikerton and Wilson, 1994). The four long Quaternary basaltic flows exhibit inflation structures such as lava rises and/or tumuli and in some cases lava tubes such as in the Toomba and Undara flows (Stephenson et al., 1998) that insulate the lava, thereby reducing its cooling by <50°C/100 km according to the models of Keszthely and Self (1998). Of special interest is the Pampas Onduladas flow as it has been described as the longest on Earth during the Quaternary (Pasquarè et al., 2008). It has a relatively narrow (~5 km) tongue-like structure that dominates for more than 70% of its length and lacks lava tube structures.

Despite the significance of the Pampas Onduladas flow, rheological, geochemical and geochronological analyses are lacking. Previous investigations mainly dealt with recognising and describing this flow from a morphological view point (Pasquarè et al., 2005; Pasquarè et al., 2008). The purpose of this investigation is to assess some of the physical parameters and geochemical characteristics of this flow, in order to comprehend the factors that have facilitated its length, and to also determine the eruption age.

2 Background

2.1 Regional geological setting

The Andean volcanic arc occupies the western margin of South America and is dominated by andesitic lavas with abundant pyroclastic ejecta. This volcanism mainly results from the dehydration of the subducting oceanic plate to the west of the South American plate (Thorpe, 1984). The subducting oceanic plates are the Nazca plate from ~5°N to ~46°S and the Antarctic plate from ~46°S. The volcanic arc is not continuous along the Andes as in areas of flat (sub-horizontal) subduction volcanic activity is absent. The Nazca plate subducts at a shallow angle long the Peruvian and the Pampean flat slab segments constituting the divide between the Northern and Central volcanic zones and between the Central and the Southern volcanic zone, respectively (Stern, 2004). The Southern and Austral volcanic zones are separated by the Chile rise which constitutes the boundary between the Nazca and the Antarctic plates.

Despite the abundance of arc volcanism, alkali basaltic volcanism also occurs behind the main Andean volcanic arc, this volcanism is termed continental back-arc volcanism. In this setting, the subduction signature decreases in an easterly direction from the arc (Stern et al., 1990; Rivalenti et al., 2004; Jacques et al., 2013). A high density of continental back-arc volcanism is found in the Southern volcanic zone mainly due to changes in subduction regime (Kay et al., 2006). The current investigation is based on the northernmost back-arc basaltic province from the Southern volcanic zone called the Payenia Basaltic Province (PBP), defined by Polanski (1954) (also described as the Andino-Cuyana Basaltic Province by Bermúdez and Delpino, 1989). The PBP covers an area of approximately 40,000 km^2, with more than 800 volcanic cones, the majority of them being monogenetic (Ramos and Folguera, 2011). The PBP is classified into several volcanic fields (Figure 1) including Nevado, Llancanelo, Payún Matrú and Rio Colorado (Ramos and Folguera, 2011; Gudnason et al., 2012) mostly based on their geochemical diversity. In this sense, the Nevado volcanic field has a defined subduction signature while the Rio Colorado volcanic field has a typical intraplate signature resembling that of ocean island basalts (Kay et al., 2013; Søager et al., 2013). The Llancanelo volcanic field has weak subduction signature while the same type of signature was not recognised in the Payún Matrú Volcanic Field (PMVF; Espanon et al., 2014). The basalts from the Payún Matrú volcanic field have an intraplate geochemical signature similar to that of the Rio Colorado volcanic field (Espanon et al., 2014). The Pampas Onduladas flow is part of the PMVF and is located on the eastern side of this volcanic field where the oldest basaltic flows are found (Figure 1). The PMVF covers an area of 5200 km^2 and is located approximately 400 km from the trench and 140 km to the east of the Andean volcanic arc (Inbar and Risso, 2001).

2.2 Payún Matrú volcanic field (PMVF) and Pampas Onduladas flow

The back-arc volcanism in the PMVF is associated with an enriched mantle similar to an ocean island basalt-type (Kay et al., 2004; Germa et al., 2010; Søager et al., 2013) associated with an intraplate setting comparable to the Rio Colorado volcanic field (Figure 1). The volcanic cones in the PMVF are mainly aligned in an E-W direction corresponding to La Carbonilla Fracture (Figure 1; Llambías et al., 2010). This fracture was formed by crustal relaxation after a period of compression associated with flat subduction during the Miocene (Kay et al., 2006). La Carbonilla Fracture is exposed in its eastern part, interrupted by the Payún Matrú caldera in its central part (Figure 1) and completely covered along its western part (inferred to underlie a field of aligned scoria cones; Hernando et al., 2014). The Pampas Onduladas flow is located on the eastern side of the PMVF (Figure 1) and its eruption point is associated with the far eastern end of La Carbonilla Fracture.

As volcanic activity continues, younger flows generally cover older flows. For example, the Thorsa long flow (~140 km) in Iceland constitutes a more recent (Holocene) example where the source craters have been covered by successive lava flow (Halldorsson et al., 2008). The eastern end of La Carbonilla fracture has been one of the major feeding systems for basaltic flows in this sector and has been active since probably the early Quaternary (Pasquarè et al., 2008). The oldest basalts erupted from La Cabonilla fracture pre-date the formation of the Payún Matrú caldera (Llambías et al., 2010; Hernando et al., 2012) which were then partially covered by the ignimbrite during the caldera formation stage and later partly overlain by younger basaltic flows. Despite the difficulty in determining the eruption point for the extensive Pampas Onduladas flow, it has been assigned to La Carbonilla fracture (Núñez, 1976; Pasquarè et al., 2005; 2008). The basement beneath the Pampas Onduladas flow is composed of older basaltic flows from the mid to late Miocene Palauco Formation (Narciso et al., 2001) and with a thickness ranging from 150 m to 800m (Méndez et al., 1995).

The volcanism in the PMVF is understood to be older on its eastern side; however, the geochronology is poorly constrained. Flows from the eastern side of the PMVF have reported K-Ar ages ranging from 600 ± 100 ka (2σ) (Berttoto, 1997) to 950 ± 500 ka (2σ) (Núñez, 1976). A single age estimate comes from a basaltic flow located stratigraphically below the Pampas Onduladas flow dated to 400 ± 100 ka (2σ) by K-Ar (Melchor and Casadio, 1999). Furthermore, the Pampas Onduladas flow pre-dates the Payún Matrú caldera (Figure 1) as the Portezuelo Ignimbrite stratigraphically overlies the Pampas Onduladas flow. The caldera-forming event is recognised to have occurred between 168 ± 4 ka and 82 ± 2 ka based on K-Ar dating (Germa et al., 2010), providing a minimum age constraint for the Pampas Onduladas flow. Therefore, its age is possibly younger than 400 ka and older than 168 ka.

The Pampas Onduladas flow as well as most of the older flows in the PMVF, has a pahoehoe character, in contrast to the younger flows (<10 ka), which are dominated by a'a morphology (Inbar and Risso, 2001; Figure 2). The Pampas Onduladas flow has been described by Pasquarè et al. (2005; 2008) as a compound flow, having an external morphology dominated by tumuli and lava rises, which are typical of an internally inflated flow. The tumuli are elongated in the medial area, while in the distal areas elongated lava rises are abundant (Figure 3). The appearance of the tumuli (~40km from the initial part) is similar to those described in the Llancanelo volcanic field (Nemeth et al., 2008) as they are flow-lobe tumuli generally less than 9 metres in height with relatively steep angles and a central crack from which lava outpour was not recognised (Figure 3). The lava rises are randomly oriented long the flow and with a range of dimensions and they generally have a central cleft (Figure 3). Lava rises are recognised on the side of the kipukas (Figure 3) in the proximal to medial section of the flow where higher pre-existing topography was engulfed by the flowing lava. The internal structure is composed of a thin, highly vesicular crust, which is on average less than 1 metre thick and the vesicles are rounded to subrounded with a maximum diameter of 2 cm. This upper zone is underlain by a dense layer in some parts heavily jointed which is approximately 2-3 m thick (Pasquarè et al., 2008). Below this layer, the jointing diminishes and the lava is more vesicular (elongated aligned vesicles), gradually changing to a massive layer formed by co-mingling of the elongated vesicles (Pasquarè et al., 2008). The flow has a hawaiite composition with low phenocryst content (Figure 4; Pasquarè et al., 2008).

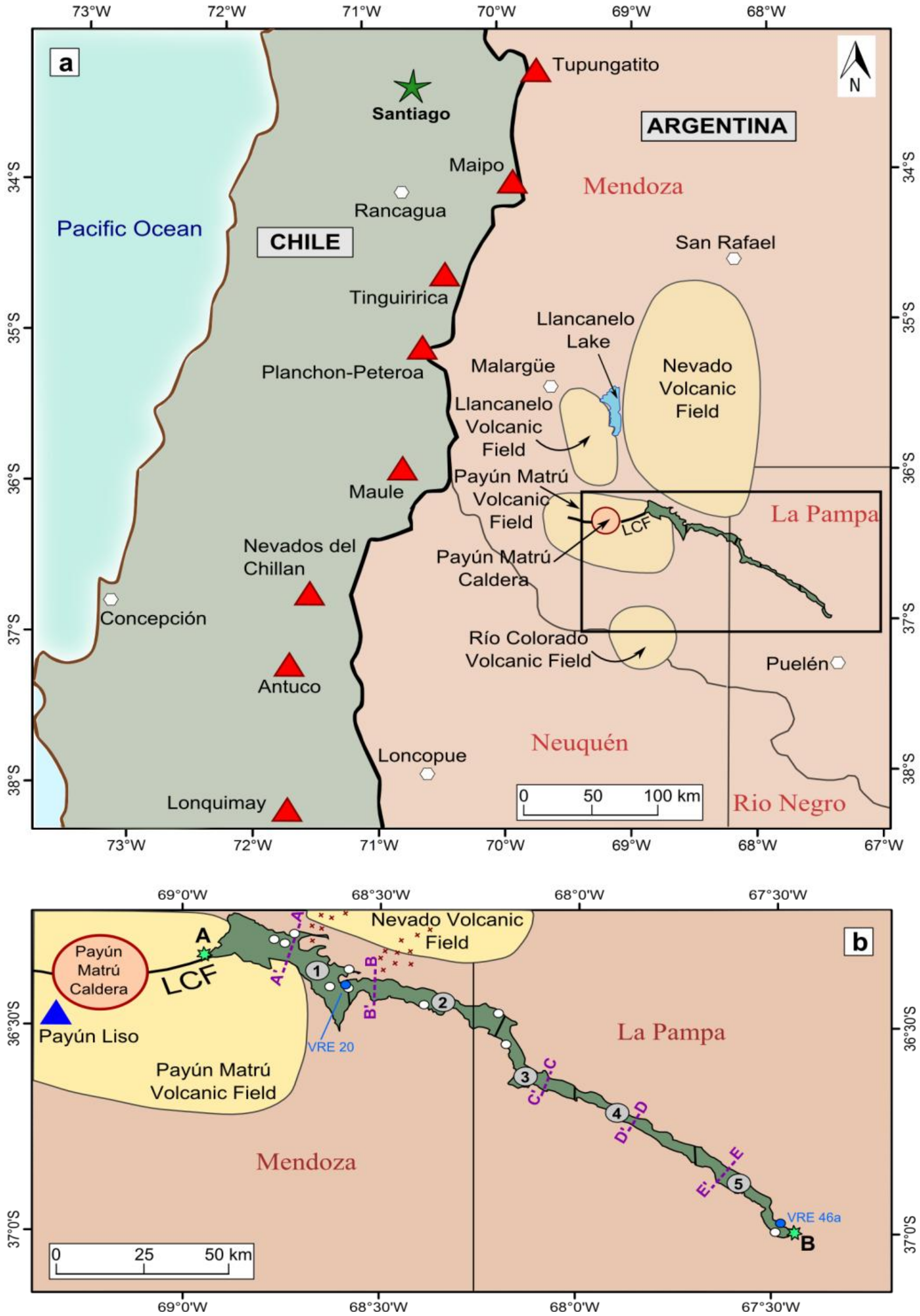

Figure 1: a) Geographical setting of the Pampas Onduladas flow. LCF indicates La Carbonilla Fracture in the Payún Matrú Volcanic Field (PMVF). The hexagons are towns. Red triangles are volcanoes from the Andean arc. b) Map of the southern Mendoza region with the Pampas Onduladas flow in green. The numbers on the Pampas Onduladas flow indicate sections 1 to 5 into which it has been divided. Dashed purple lines indicate the location of each of the cross sections (refer to Figure 5). The red crosses indicate exposures of the San Rafael Block. The white circles within the flow are samples from Pasquarè et al. (2008) and from Espanon et al. (2014), while the two blue circles are the samples used for $^{40}Ar/^{39}Ar$ dating. The two green stars (A and B) represent the initial and final points of the flow; between which the length was calculated.

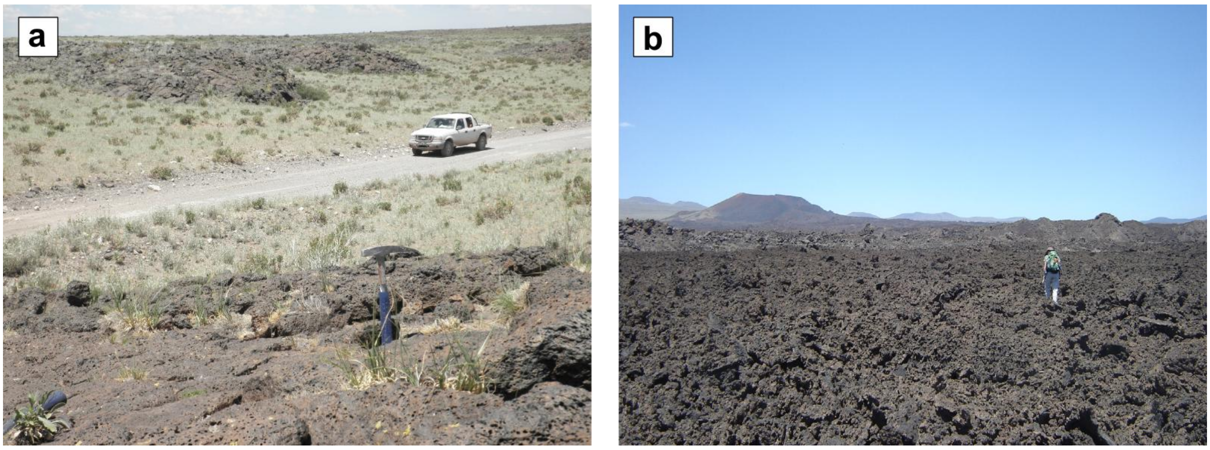

Figure 2: Examples of basaltic morphotypes from the Payún Matrú volcanic field. a) Proximal to central part of Pampas Onduladas flow, showing a pahoehoe morphology; b) Proximal to central part of Santa Maria flow, showing an a'a morphology. Note the smooth surface of the pahoehoe Pampas Onduladas flow in contrast to the rough surface of the Santa Maria flow.

The magmatic source region for this extensive flow has been inferred to be affected by metasomatism associated with the subduction of the Nazca plate (Pasquarè et al., 2008), although recent studies suggest that the Payún Matrú Volcanic Field (PMVF, Figure 1) shows minimal (Jacques et al., 2013; Søager et al., 2013) to negligible (Espanon et al., 2014) evidence for subduction signatures. The basalts in the PMVF have geochemical characteristics similar to the local ocean island basalt (OIB) source (Espanon et al., 2014), taken as the Rio Colorado Volcanic Field previously described by Søager et al. (2013) as OIB-type. In addition, lower crustal assimilation has been suggested (Espanon et al., 2014) for the Pampas Onduladas flow.

3 Methods

Available geochemical data from the Pampas Onduladas flow are summarised in Table 1 (Pasquarè et al., 2008; Espanon et al., 2014). The extent of the Pampas Onduladas flow was determined using existing maps (Pasquarè et al., 2008) as well as a digital elevation model and surface maps. The length was calculated along the medial axis of the mapped flow from the inferred eruption and terminal points (Cashman et al., 2013). The eruption point is inferred to be close to the eastern limit of La Carbonilla fracture (point A; Figure 1) while the inferred terminal point is located in the province of La Pampa (point B; Figure 1) with the following geographical coordinates: 36.33778°S, 68.93918°W, 1852 MASL (Point A); and 37.00509°S, 67.45564°W, 445 MASL (Point B).

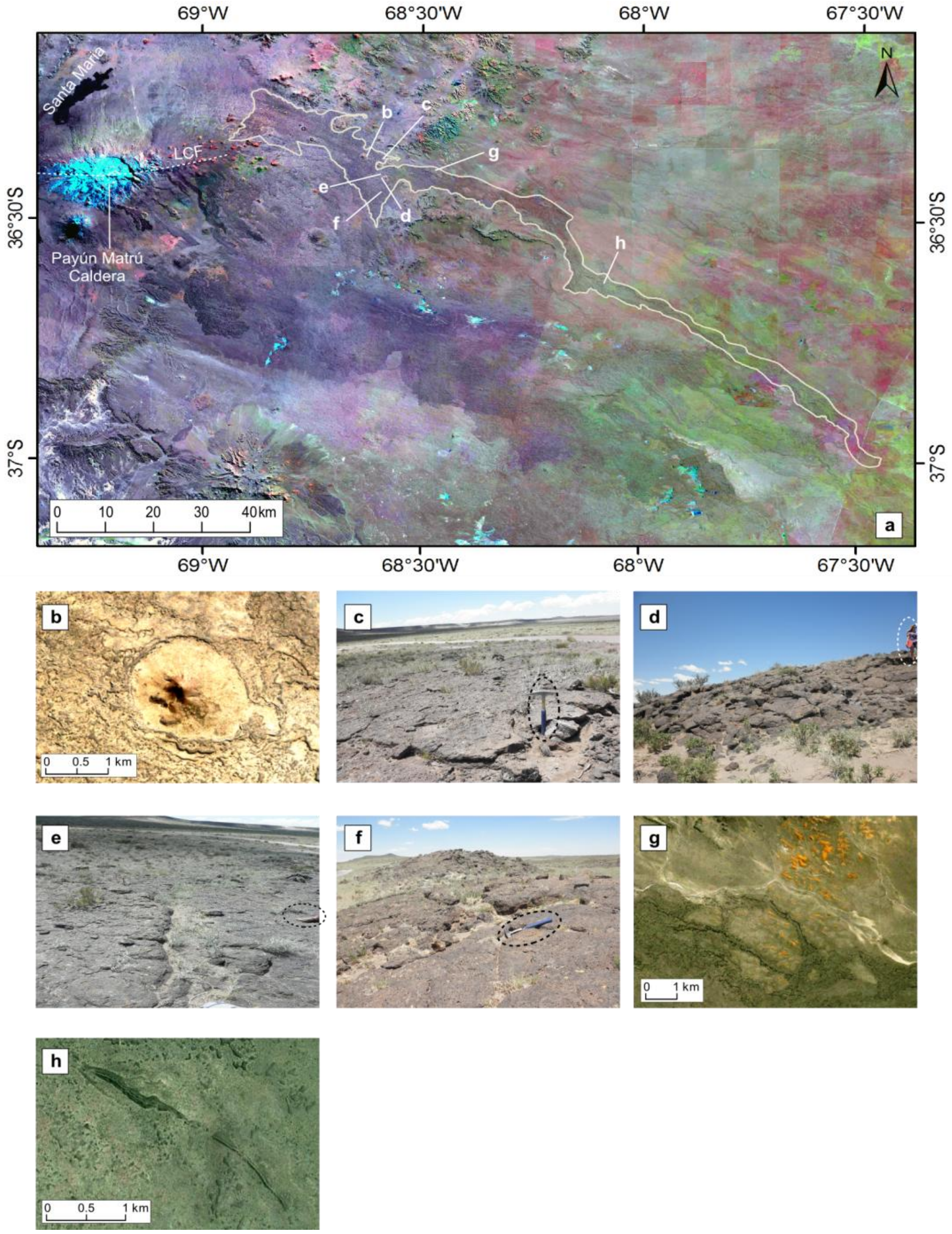

Figure 3: Morphological structures along the Pampas Onduladas flow. a) Outline of Pampas Onduladas flow showing the location for images b) to h). b) One of several kipukas located in the proximal-medial part of the flow. Note how the basaltic flow engulfed the pre-existing volcanic cone forming lava rises. c) Slabby pahoehoe flow; note the highly vesicular top layer. Geological hammer for scale is 32 cm long. d) Side view of a basaltic tumulus. Person on the right for scale. e) Groove on the surface of Pampas Onduladas flow. Note circled shoe for scale ~ 28 cm. f) view of a Pampas Onduladas surface and a tumulus in the background. Note the central crack in the tumulus. g) View of several kipukas in the northern margin of Pampas Onduladas. The pre-existing topography is part of the San Rafael block and the flow has formed lava rises in the margins of the kipukas. h) longitudinal lava rise with a central groove. The base satellite photo for a) is a mosaic contrast sharpening from preview images LC82300862013145LGN00, LC82310852013168LGN00, LC82310862013136LGN01 and LC82300852013145LGN00 from Landsat 8.

3.1 $^{40}Ar/^{39}Ar$ geochronology

Two samples were collected for $^{40}Ar/^{39}Ar$ geochronological analysis; sample VRE20 from the initial to medial part of the flow (36.40847°S, 68.58000°W), and sample VRE46a from the lower end of the flow (36.97117°S, 67.49233°W) (Figure 1). These samples are fine-grained, hypocrystalline alkali basalts with 1.0 wt % K_2O (VRE20) and 0.9 wt % K_2O (VRE46a), respectively (petrographic descriptions are provided in Section 4.1 and Figure 4). Following procedures described in Matchan and Phillips (2014), sample preparation involved crushing approximately 300 g of whole-rock to a grain-size of 180-250 μm followed by magnetic separation and hand picking to isolate unaltered groundmass from the phenocrysts. The groundmass separate and the neutron flux monitor Alder Creek Rhyolite (ACR) sanidine (1.186 ± 0.012 Ma (1σ); Turrin et al., 1994) were irradiated at the USGS TRIGA reactor for 0.5 MWH in the Cd-lined facility. Irradiated samples and the ACR flux monitor were analysed in the School of Earth Sciences at the University of Melbourne using a multi-collector Thermo Fisher Scientific ARGUSVI mass spectrometer linked to a gas extraction/purification line and Photon Machines Fusions 10.6 μm CO_2 laser system (Phillips and Matchan, 2013), following procedures described by Matchan and Phillips (2014). Blanks were measured after every third analysis and yielded <2.9 fA for ^{40}Ar, corresponding to 0.21% of the measured ^{40}Ar in the experiments. Mass discrimination was determined by automated air pipette aliquots before analysis assuming an atmospheric $^{40}Ar/^{36}Ar$ of 295.5 ± 0.5 (Nier, 1950). The ages were calculated relative to the ACR flux monitor, which determines the production of ^{39}Ar from ^{39}K during the radiation process and the ^{40}K decay constant of 4.962 x 10^{-10} yr^{-1} (Steiger and Jäger, 1977).

Table 1: Major- and trace-element analysis of the Pampas Onduladas flow. The major-elements are in wt % and the trace elements are in ppm. The major-elements are recalculated to an anhydrous basis (original data Pasquarè et al., 2008; Espanon et al., 2014).

Sample	**VRE19**	**VRE20**	**VRE21**	**VRE46 (A)**	**VRE47**	**PY16**	**PY20**
Latitude(°)	-36.4124	-36.4085	-36.3732	-36.9712	-36.9987	-36.3939	-36.2919
Longitude(°)	-68.5789	-68.5800	-68.5754	-67.4923	-67.4992	-68.6413	-68.7628
SiO_2	47.16	48.22	49.51	49.01	48.86	47.82	47.73
TiO_2	1.97	1.96	1.91	1.78	1.54	1.63	1.65
Al_2O_3	17.36	17.45	18.09	17.23	16.30	17.88	18.28
FeO_t	11.78	11.49	10.75	11.55	11.98	10.86	10.03
MnO	0.15	0.15	0.15	0.15	0.15	0.14	0.16
MgO	7.21	6.94	5.90	7.01	8.82	7.91	7.61
CaO	8.91	8.79	8.61	8.75	8.01	8.36	9.53
Na_2O	3.93	3.50	3.23	3.24	3.39	3.82	3.27
K_2O	1.04	1.01	1.33	0.89	0.67	1.04	0.84
P_2O_5	0.48	0.49	0.48	0.38	0.27	0.39	0.32
V	221	225	242	221	186	133	192
Cr	197	190	244	247	293	298	196
Ni	81	77	105	144	216	109	73
Rb	14.5	14.8	22.8	12.7	9.5	18.0	15.0
Sr	642	638	626	557	367	600	587
Y	23.5	23.1	22.6	20.8	18.4	16.0	16.0
Zr	148	149	199	135	104	123	123
Nb	19.0	19.3	22.3	13.6	9.5	15.0	14.0
Cs	0.3	0.3	0.3	0.2	0.2	0.3	0.5
Ba	308	475	510	320	183	305	356
La	18.7	18.4	20.4	14.0	10.7	14.9	16.0
Ce	37.6	36.0	34.4	28.6	22.6	31.5	34.7
Pr	5.0	4.9	5.1	3.9	3.1	3.9	4.5
Nd	23.2	22.4	23.3	18.5	14.7	17.3	20.1
Sm	5.6	5.5	5.6	4.8	4.0	4.3	5.0
Eu	1.9	1.8	1.8	1.7	1.4	1.6	1.8
Gd	5.5	5.4	5.3	5.0	4.1	4.3	4.9
Tb	0.9	0.8	0.9	0.8	0.7	0.7	0.8
Dy	4.9	4.7	4.6	4.3	3.8	3.9	4.4
Ho	0.9	0.9	0.9	0.8	0.7	0.7	0.9
Er	2.5	2.4	2.4	2.2	2.0	1.9	2.3
Tm	0.3	0.3	0.3	0.3	0.3	0.3	0.3
Yb	2.1	2.1	2.1	1.9	1.6	1.5	1.8
Lu	0.3	0.3	0.3	0.3	0.2	0.2	0.3
Hf	3.7	3.7	4.9	3.4	2.7	2.5	3.3
Ta	1.1	1.1	1.4	0.8	0.5	0.7	0.7
Pb	3.5	3.4	4.8	3.8	2.6	3.0	
Th	2.0	2.0	3.2	1.7	1.3	1.5	1.6
U	0.5	0.5	0.8	0.5	0.3		0.5

Table 1 cont

Sample	**PY23**	**PY24**	**PY25**	**PY34a**	**PY34b**	**SAL1**	**SAL4**
Latitude(°)	-36.4597	-36.4721	-36.5541	-36.9702	-36.9702	-36.2764	-36.2944
Longitude(°)	-68.3886	-68.1894	-68.1754	-67.4913	-67.4913	-68.7088	-68.7316
SiO_2	47.56	47.25	47.86	48.75	47.25	48.86	47.86
TiO_2	1.9	1.83	1.77	1.73	1.49	1.85	1.78
Al_2O_3	17.53	17.2	17.56	17.49	16.83	16.48	16.2
FeO_t	10.74	10.65	11.15	10.65	10.81	11.21	11.1
MnO	0.16	0.16	0.16	0.16	0.18	0.17	0.16
MgO	6.87	7.35	7.3	7.62	9.14	6.96	7.05
CaO	9.5	9.39	8.96	8.75	9.32	9.78	10.17
Na_2O	3.47	3.5	3.46	3.5	3.43	3.74	3.61
K_2O	1.01	0.91	0.93	0.86	0.82	1.28	1.22
P_2O_5	0.37	0.35	0.35	0.29	0.26	0.44	0.44
V	179	187	188	152	197	210	217
Cr	221	256	256	247	417	240	220
Ni	82	97	103	115	190	110	110
Rb	15.0	15.0	15.0	14.0	18.0	23.0	26.0
Sr	583	571	564	553	518	627	621
Y	16.0	16.0	18.0	15.0	16.0	21.6	23.5
Zr	130	124	125	119	118	151	144
Nb	18.0	17.0	17.0	14.0	11.0	16.2	15.1
Cs	0.3	0.3	0.4	0.3	0.7	0.7	0.8
Ba	293	257	251	238	298	303	443
La	17.7	16.9	16.6	14.4	16.2	19.0	19.1
Ce	37.8	36.2	36.1	30.9	35.0	40.2	40.8
Pr	4.6	4.5	4.4	3.9	4.4	5.1	5.4
Nd	20.9	20.0	20.5	17.5	19.5	20.9	21.6
Sm	5.0	4.9	5.1	4.5	4.8	5.1	5.4
Eu	1.8	1.8	1.9	1.6	1.7	1.8	1.9
Gd	4.9	4.8	5.0	4.4	4.5	4.8	5.1
Tb	0.8	0.8	0.8	0.7	0.8	0.8	0.8
Dy	4.4	4.4	4.5	4.0	4.2	4.5	4.5
Ho	0.8	0.8	0.8	0.7	0.8	0.8	0.8
Er	2.2	2.2	2.2	2.0	2.1	2.2	2.3
Tm	0.3	0.3	0.3	0.3	0.3	0.3	0.3
Yb	1.8	1.7	1.8	1.6	1.8	2.0	2.0
Lu	0.3	0.3	0.3	0.2	0.3	0.3	0.3
Hf	3.4	3.2	3.3	3.0	3.1	3.6	3.6
Ta	1.0	1.0	0.9	0.7	0.6	1.3	1.1
Pb	2.0	2.0	1.0		6.0		
Th	1.7	1.6	1.6	1.4	2.3	3.0	2.7
U	0.5	0.5	0.5	0.4	0.7	0.7	0.7

3.2 Rheological characterisation

The rheological parameters were calculated using the Magma® program from K. Wohletz (www.ees1.lanl.gov/Wohletz/Magma.htm). This program uses the major-element composition, crystal volume and crystal or vesicle size to calculate the density, liquidus temperature and viscosity of lava flows. The following values are used based on petrographic observations: phenocryst volume = 15 %; and crystal or vesicle maximum average size = 5 mm. The phenocrysts volume is based on hand specimens and photomicrograph observations (Figure 4) showing low phenocryst content as also noted by Pasquarè et al. (2008). The vesicle size is based on an average from field observations (Figure 3b, e) and hand specimens (Figure 4). Magma® calculates the liquidus temperature based on the method of Sisson and Grove (1993) and the density based on the method described by Bottinga and Weil (1972). A 20% vesicle volume correction (average vesicle volume of Pampas Onduladas flow) was applied to the density calculation which also correlated with observations from other large basaltic flows (Keszthelyi and Pieri 1993). The parameters here used to calculate the viscosity (15% phenocryst volume, 5mm phenocryst or vesicle size and 20% vesicle volume) are based on field observations. It is important to consider that the exposed part of the Pampas Onduladas flow is the uppermost highly vesicular layer (Figure 4a) which does not fully represent the characteristic of the long flow, therefore the values used were also correlated with those presented by Pasquarè et al. (2008) and other estimates on long lava flows (Keszthelyi and Self, 1998). The viscosity was calculated using Magma® and the algorithms proposed by Bottinga and Weil (1972). Furthermore, the flow velocity was calculated using Jeffrey's Law equation:

$$v = \frac{\rho\ g\ \theta\ H^2}{8\eta}$$

where ρ is the density of the flow (in kg/m^3), g is the gravitational acceleration (9.8 m/s^2), θ is the slope (0.0084), H is the thickness (variables used: 20m, 15m, 10m and 5m) and η is the viscosity (in Pa.s). The 20m thick variable used is based on, the preserved Pampas Onduladas thickness above the surrounding topography (Figure 5) which also corresponds to the minimum thickness proposed by Pasquarè et al. (2008). However, the 20m thick variable is the preserved thickness of the flow after inflation and cooling, therefore it does not represent the original thickness. In order to account for the velocity several hypothetical thickness values of less than 20m, were chosen at regular set intervals.

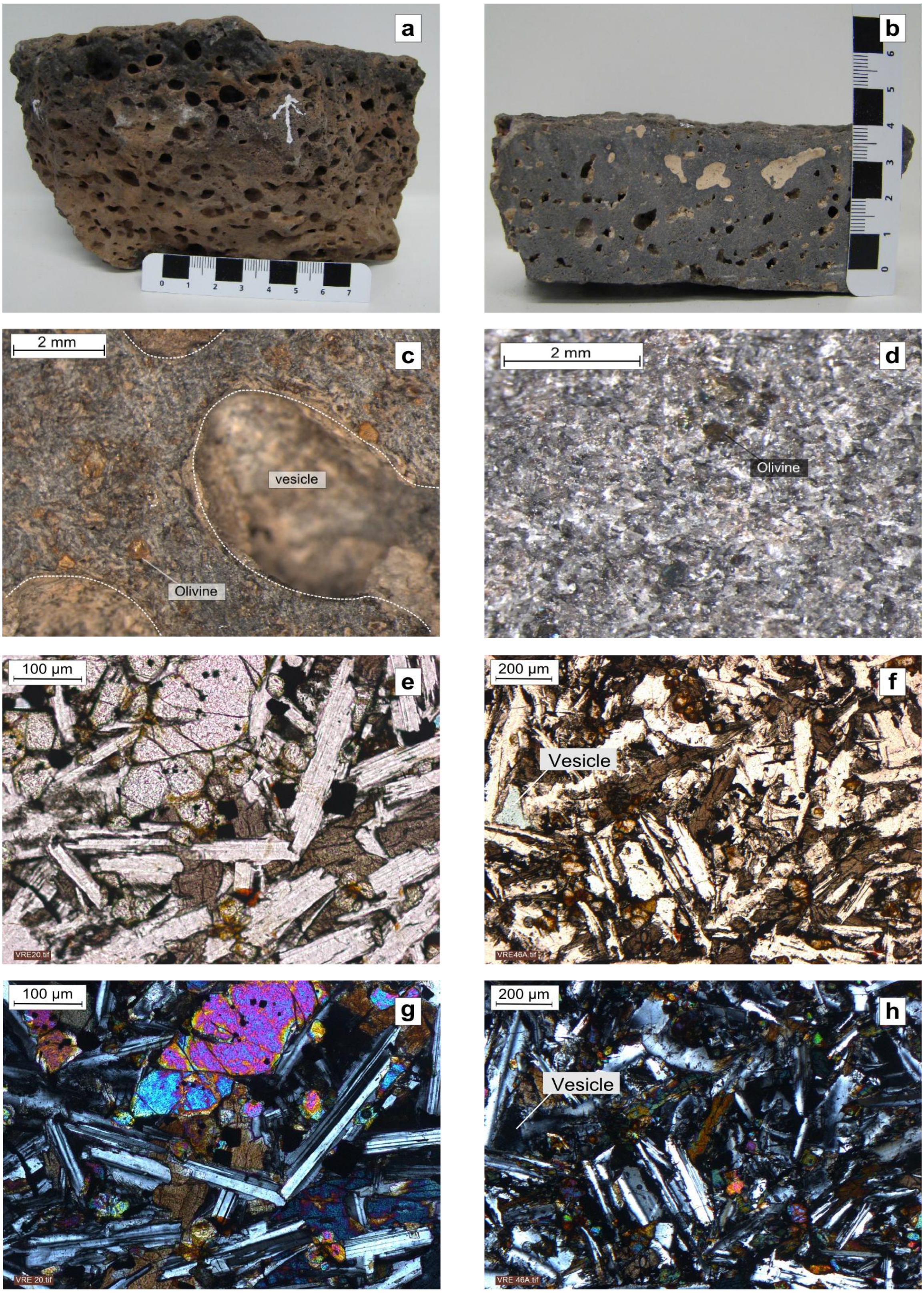

Figure 4: Images of samples from the Pampas Onduladas flow. a) Sample VRE20 uppermost layer. White arrow indicates way up, note the roundness of the vesicles (scale in cm and mm). b) Sample VRE46a uppermost layer. Note the vesicles are not rounded and some are filled by carbonates. c) photomicrograph of a cut surface of sample VRE21. d) photomicrograph of the surface of sample VRE46a showing the high crystal content of the rock. e) and f) polarised photomicrographs of samples VRE20 and VRE46a, respectively. g) and h) cross-polarised photomicrographs of samples VRE20 and VRE46a, respectively.

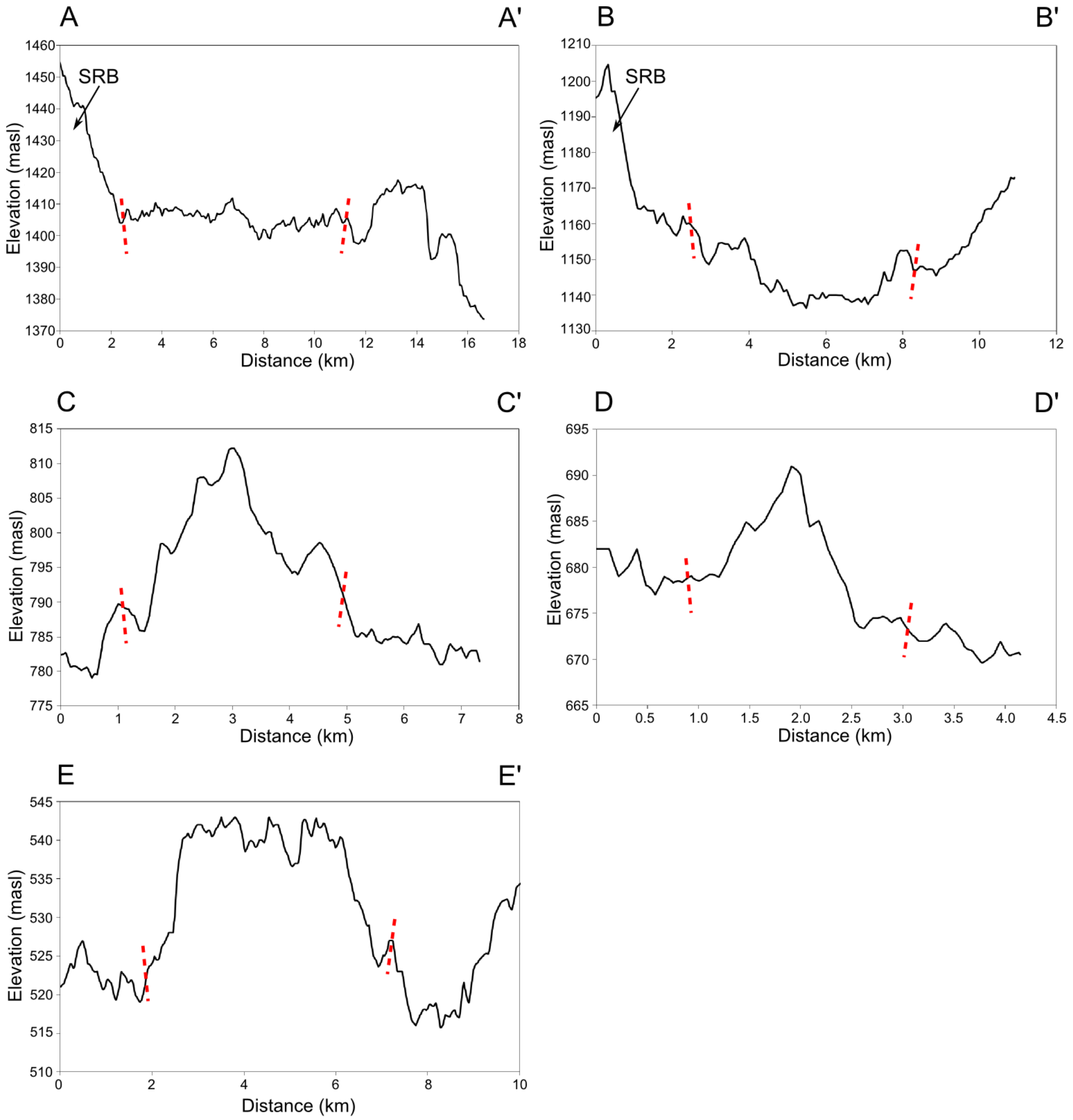

Figure 5: Cross sections of the Pampas Onduladas flow. North is to the left in each case and the vertical scale is exaggerated. Cross sections a) to e) correspond to sections 1 to 5 of the flow. Red dashed lines in each of the cross sections delimit the margins of the Pampas Onduladas flow. The San Rafael block (SRB) outcrops on the northern side of cross sections A-A' and B-B'.

3.3 Volume Calculation

The topographic slope was calculated using the difference in elevation from the initial point A (1852 MASL) to the final point B (445 MASL) divided by the total calculated length of the flow. The elevation of points A and B and volume calculation were based on the digital elevation model (DEM), Shuttle Radar Topography Mission (SRTM) 90 m (30m x 30 m) with an absolute vertical error of less than 9 m and a relative vertical error of less than 10 m (Rodriguez et al., 2006). Five cross-sections (Figure 1) were made along the flow in order to assess the topographic correlation between the flow and the adjacent pre-existing surfaces, as well as to estimate its thickness. The volume was calculated using the procedure described by Smith et al. (2009) based on the SRTM digital elevation model and employing the ArcGIS® software. To calculate the volume, the Pampas Onduladas flow was divided into 5 segments (Figure 1) in order to account for the changes in slope and adjacent topography. The volume was calculated for each individual segment and then summed to provide the total. There are areas of the flow, especially in its proximal part, where it is interrupted by the pre-existing topography (kipukas) such as scoria cones and elevated landscapes (i.e. parts of the flow where the underlying substrate has not been covered; Figure 3a, f). The volumes of each of the kipukas was calculated and later subtracted from the total (see following section for further details). The errors associated with the volume calculations have not been determined as this is a first-order estimate of the volume (see Smith et al., 2009) and there are several potential sources of error that are difficult to quantify. The possible sources of error include: (i) the SRTM has an absolute height error of less than 9 m in a global scale and 6.2 m for South America (Rodriguez et al., 2006); (ii) digitalisation is based on user interpretation; (iii) topographic highs on the sides of the flow may give inaccurate base surfaces; and (iv) data point interpolation. The interpolation algorithm uses the values from the sides of the flow to create a planar estimate of the underlying surface; however the interpolation does not consider topographic lows that may have existed before the lava emplacement.

3.3.1 Detailed volume calculation method

The volume was calculated by modifying the approach of Smith et al. (2009). The procedure used is described in several steps.

1- The Pampas Onduladas flow was digitised using Landsat7 imagery Google Earth® and then divided into 5 segments. In addition, features such as kipukas, were also digitised.

2- The files created where exported to ArcGIS10® and the remaining analyses were performed using this software. The volume was calculated individually for each sector and kipuka. The total volume was determined by summing all the sector volumes. The same principle was applied to all the kipukas. Finally, the total volume of the kipukas was subtracted from the total volume.

3- The SRTM 90m (30 m x 30 m) digital elevation model covering the area of interest was uploaded to ArcGIS10®. Using the Windows tool, selecting the sector shapefile and employing the create-a-void command a cavity covering the area of the sector was created in the DEM. Basically, in this step, the sector of the flow being calculated was removed from the DEM. The same principle was applied for the kipukas.

4- After removing the sectors, the surrounding topography was interpolated to create an approximate base surface. In order to do this, all the values of each cell in the SRTM were converted to point values using the conversion tool. Once the new point layer was created, interpolation between point values was carried out. The interpolation tool used is the spline (Smith et al., 2009) and the output cell size was set with the default value for sector 1. The default value used for sector 1 was then used for all sectors from 2 to 5.

5- The hypothetical basal surface created, was isolated from the rest of the DEM. This was done using the Windows tool and employing the clip option. The resulting layer should only contain the interpolated base area of the sector. The same principle was applied to the original DEM so that the top surface of the sector was isolated from the rest of the DEM.

6- Once the base and top part of a particular section were isolated, the volume and area of the top and the base surface were calculated separately using the Area and Volume statistics option. In the calculation, the plane height differed from sector to sector as they have different elevations; therefore the default value for each particular sector was used. The calculated volume and area from the top and base of the sector were exported into Excel.

7- The final volume of each sector was calculated using Excel by subtracting the base volume from the top volume. The volume from the 5 sectors was summed and the volume from the kipukas that interrupted the Pampas Onduladas flow was subtracted.

4 Results

4.1 Petrographic description of Pampas Onduladas Flow

The Pampas Onduladas samples are highly vesicular in the uppermost layer (Figure 4) with well developed roundness in the proximal-middle part of the flow (Figure 4a) while the vesicles are longitudinally deformed in the distal part (Figure 4b). Nevertheless, a sub-angular vesicle can be observed in sample VRE46a (Figure 4f and h). The rocks from the flow are fine grained and hypocrystalline (Figure 4c and d) with sparse phenocrysts; the groundmass is composed of microliths. The photomicrographs show a subophitic texture for sample VRE20 (Figure 4e and g), which is generally found in the central part of basaltic flows (Llambías, 2008). Sample VRE46a has an interstitial texture (Figure 4f and h). The rocks are mainly composed of plagioclase, olivine, and orthopyroxene with some clinopyroxene (Figure 4g, h). Olivine phenocrysts are euhedral to subhedral, and some of show alteration on the margins to iddingsite. All the samples contain opaque minerals.

4.2 Ar-Ar results

A summary of the results from the $^{40}Ar/^{39}Ar$ analysis is shown in Table 2 (including plateau, inverse isochron and total gas ages) and Figure 6, while the full data set is presented in Supplementary Data 1. Plateau age plots (Figure 6a), step heating spectra (Figure 6b) and inverse isochron graphs were produced using the Isoplot 3.75 add-in for Microsoft Excel (Ludwig, 2012).

The age spectrum for VRE20 comprises an essentially flat profile followed by successively older apparent ages for high-temperature steps. A plateau age of 373 ± 10 ka (2σ) was calculated for sample VRE20 (Table 2), using the plateau criteria of Singer and Pringle (1996). The slightly higher apparent age calculated for the initial step most likely reflects release of excess ^{40}Ar from fluid inclusions at low temperature. The older apparent ages calculated for the high temperature steps most likely reflect outgassing of incompletely removed plagioclase and clinopyroxene phenocrysts, consistent with elevated Ca/K ratios and observations in other whole-rock basalt $^{40}Ar/^{39}Ar$ studies (e.g. Cassata et al., 2008). An inverse isochron generated for all data, excluding the anomalous result from the final fusion step, suggests a trapped argon component ($^{40}Ar/^{36}Ar_i$) with a near-atmospheric composition of 299.2 ± 2.9 (95% CI; MSWD = 5.5). However, the high MSWD of this fit reflects the discordance of the data, indicating the presence of at least two trapped argon components. A well-constrained atmospheric $^{40}Ar/^{36}Ar_i$ ratio of 296.6 ± 1.7 (2σ; MSWD=1.2) is revealed by data from the plateau-forming steps (2-6), supporting the interpretation of the plateau age as an eruption/cooling age. Owing to the extremely low radiogenic $^{40}Ar^*$ concentration in this sample ($^{40}Ar^*$ comprises ~3% of total ^{40}Ar), the corresponding inverse isochron age has a poorly constrained value of 349 ± 68 ka (2σ), within error of the plateau age. The significantly older total-gas age of 434 ± 10 (2σ) reflects the extraneous $^{40}Ar^*$ released in the initial and high-temperature heating steps.

In contrast to VRE20, the age spectrum for VRE46a is highly discordant and a plateau age could not be resolved (Figure 6b). The monotonic decrease in apparent ages implicates recoil loss/redistribution of ^{39}Ar and ^{37}Ar from secondary phases and/or fine-grained magmatic phases during irradiation (e.g. Koppers et al., 2000). The older apparent ages calculated for the high-temperature steps likely reflect release of extraneous ^{40}Ar during degassing of plagioclase and clinopyroxene phenocrysts, as for sample VRE20. Due to the recoil issue apparent in this sample, inverse isochron analysis is of limited value in constraining the trapped argon composition (Koppers et al, 2000). The data are highly discordant in three-isotope space (Figure 6), but suggest a atmospheric $^{40}Ar/^{36}Ar_i$ ratio of 295.6 ± 3.0 (95% CI; MSWD=35). Therefore, assuming negligible loss of ^{39}Ar from the sample, the total gas age of 370 ± 8 ka (2σ) can be regarded as a maximum age estimate for sample VRE46a.

Table 2: $^{40}Ar/^{39}Ar$ results for groundmass samples from the Pampas Onduladas basaltic flow

Sample		**VRE20**	**VRE46a**
Flow sector		2	5
Plateau age	age (ka)	373 ± 10 (2σ)	N/A
	MSWD	1.4	N/A
	cum^{39}Ar (%)	68.2	N/A
Inverse Isochron age	age (ka)	349 ± 68 (2σ)	374 ± 76 (95% CI)
	MSWD	1.2	35
	steps included	5 of 9	9 of 9
Total-gas age	age (ka)	434 ± 10 (2σ)	370 ± 8 (2σ)

N/A not applicable

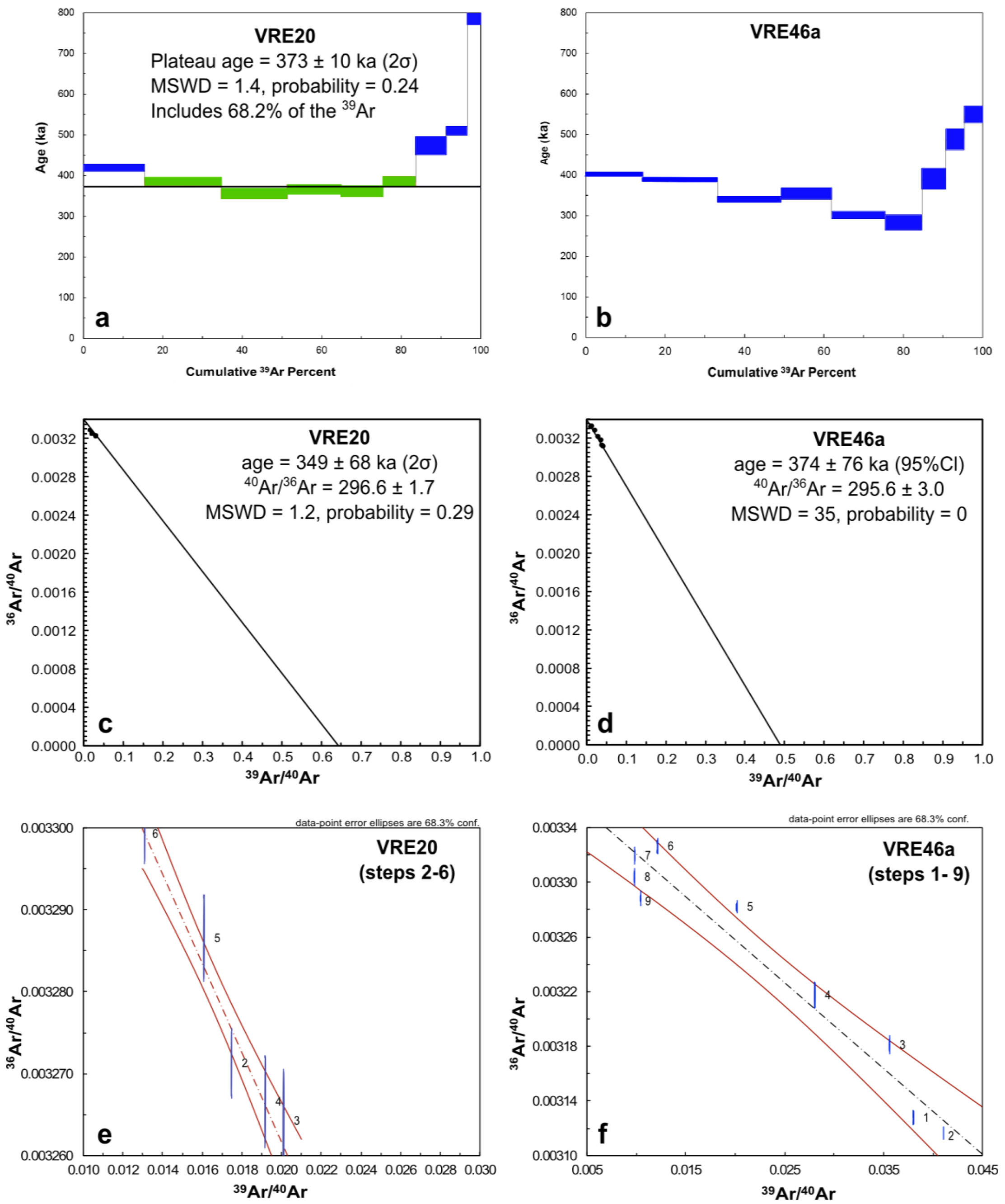

Figure 6: $^{40}Ar/^{39}Ar$ results for samples of the Pampas Onduladas basaltic flow. a) Plateau diagram for sample VRE20. b) Spectrum diagram for sample VRE46a. c) and d) Inverse isochron diagrams for samples VRE20 and VRE46a, respectively. e) and f) large-scale inverse isochron diagrams for samples VRE20 and VRE46a, respectively. The heating steps in green are those which were accepted while those in blue were rejected. Error symbols in e) and f) are 1σ.

4.3 Geochemistry of Pampas Onduladas

Major-element concentrations of the Pampas Onduladas flow suggest a primitive composition with low and restricted SiO_2 content (Table 1). The MgO content ranges from 9.1 wt % (Sample PY34b, Pasquarè et al., 2008) to 6.0 wt % (Espanon et al., 2014). The MgO concentration is negatively correlated with TiO_2, P_2O_5 and K_2O concentrations (not shown), while no correlation was established with Al_2O_3, CaO, Na_2O and FeO_t contents. A positive correlation is apparent between TiO_2 and K_2O contents (Figure 7a). Rare Earth Element (REE) concentrations normalised to the primitive mantle (values from McDonough and Sun, 1995) show enrichment in light REEs over heavy REEs (Figure 7e). This pattern is generally associated with the presence of residual garnet in the magmatic source. In addition, a small Eu peak is noticeable in Figure 7e. Trace-element concentrations, normalised to the primitive mantle (values from McDonough and Sun 1995; Figure 7f), display enrichment for Ba and Sr while some samples have a positive Pb anomaly. The negative Nb-Ta anomaly typical of arc volcanism is not apparent (except for sample PY34b, from Pasquarè et al., 2008) among samples of the Pampas Onduladas flow (Figure 7f). Sr isotope values are low, ranging from 0.703747 (Espanon et al., 2014) to 0.704151 (Pasquarè et al., 2008), which are comparable with $^{87}Sr/^{86}Sr$ values reported by Hernando et al. (2012) for pre-caldera basalts (0.703766 to 0.703906).

4.4 Rheology

The average calculated viscosity is 96 Pa.s at a mean temperature of 1170°C and with a 15% phenocryst content correction, corresponding to a typical olivine basalt melt (Williams and McBirney, 1979). The value for viscosity and temperature inferred for the Pampas Onduladas are slightly higher than the range suggested by Pasquarè et al. (2008) of 3-73 Pa.s for viscosity and 1130 - 1160°C for temperature. However, the viscosity values are within the range of those calculated for the Undara and Toomba flows in Queensland, Australia, which have a similar composition to the Pampas Onduladas flow (Stephenson et al., 1998). The calculated bulk density ranges from 2120 to 2466 kg/m^3 after correction for 20% vesicle volume.

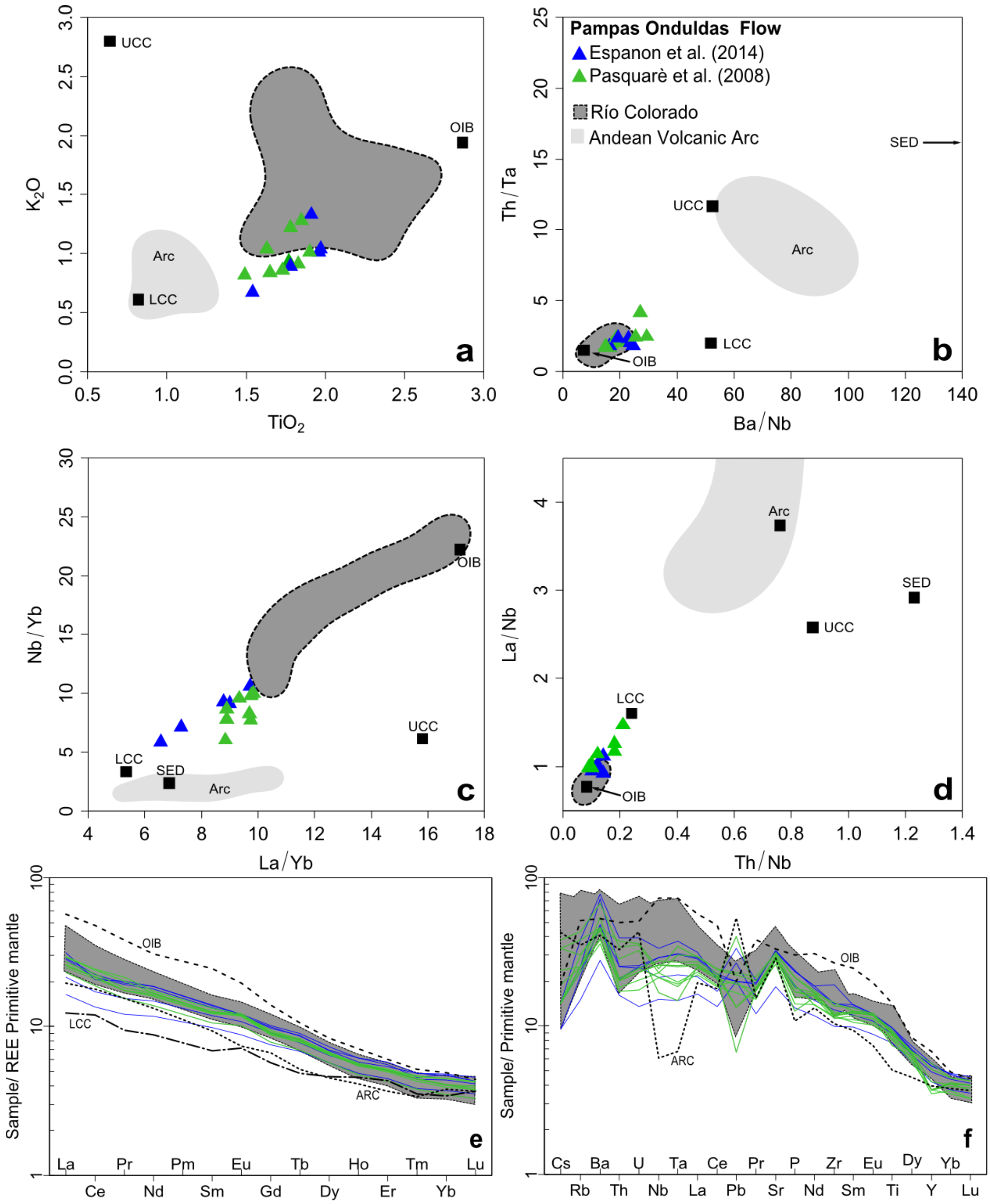

Figure 7: Geochemical data for Pampas Onduladas lavas. a) TiO_2 vs K_2O concentrations in wt %, b) Ba/Nb vs Th/Ta, c) La/Yb vs Nb/Yb, d) La/Nb vs Th/Nb, e) Rare earth element (REE) concentrations normalised to primitive mantle values (McDonough and Sun, 1995) and f) trace-element concentrations, normalised to primordial mantle values (McDonough and Sun 1995). The green triangles and lines are from Pasquarè et al. (2008), and the blue triangles and lines are from Espanon et al. (2014). The upper continental crust (UCC) and the lower continental crust (LCC) compositions are from Rudnick and Gao (2003). The ocean island basalt (OIB) composition is from Sun and McDonough, (1989). The Río Colorado volcanic field is taken as the local intraplate composition similar to an OIB endmember from Søager et al. (2013). Data from the basaltic Andean volcanic arc (ARC) are from Lopez-Escobar et al. (1977), Tormey et al. (1991) Ferguson et al. (1992), Tormey et al. (1995), Costa and Singer (2002) and Jacques et al. (2013).

The calculated velocity of the Pampas Onduladas flow (assuming a mean density value of 2300 kg/m^3) is 99 (~355 km.h^{-1}), 55, 25 and 6 m.s^{-1} for flow thicknesses of 20, 15, 10 and 5 m, respectively (Table 3). These flow velocities were calculated assuming a laminar flow behaviour. The average velocities appear excessive in comparison to the fastest velocity recorded for basaltic lava flows such as for Mt. Nyiragongo (ultramafic flow) in 1977 with speeds of approximately 17 m.s^{-1} (60 km.h^{-1}; Tazieff, 1977) or some of the Mauna Loa flows with speeds of up to 15 m.s^{-1} (55 km.h^{-1}; Lipman and Banks, 1987). Because the average velocities calculated are excessive, Reynolds numbers *(Re)* (Reynolds, 1974) were calculated to determine whether the flow was turbulent (density = 2300 kg/m^3 and viscosity = 96 Pa.s). Using velocities calculated above, *Re* values do suggest a turbulent flow (*Re* values of 47000, 20000 and 6000 at 20 m, 15 m and 10 m flow thickness; Table 3). For a 5 m thick flow, the *Re* number is 700, which is regarded as laminar. In order to calculate the velocity of a turbulent flow, a different equation must be applied that incorporates the friction coefficient (C_f) in the Chezy equation (Jeffreys, 1925) (see Appendix A for equations). Using the calculated *Re* numbers and employing the Gonacharov (1964) equation for turbulent sheet flow, a C_f value of 0.0021, 0.0025 and 0.0033 for a 20 m, 15 m and 10 m thick flow respectively were calculated. These values were incorporated into the Chezy equation to calculate the velocity of a turbulent flow: 28 (~101 km.h^{-1}), 22 (~ 79 km.h^{-1}) and 16 (58 km.h^{-1}) m.s^{-1} for a 20, 15 and 10 m thick flow, respectively (Table 3). The calculated average flow velocities are high even for a turbulent flow compared with observations from Mt Nyiragongo (Tazieff, 1977) and Mauna Loa (Lipman and Banks, 1987). Consequently some parameters were modified in order to examine the velocity change by increasing the maximum phenocryst and/or vesicle size and the vesicle volume proportion. By increasing the maximum phenocryst or vesicle size the velocity did not incur in much change (~1%) while increasing the vesicle volume to 30% the average viscosity increased to 133 Pa.s and the average bulk density decreased to 1924 kg/m^3, therefore reducing the velocity by an average of 11% which is still elevated.

Table 3: Velocity calculated at liquidus temperature for a laminar and turbulent flow, for the Pampas Onduladas flow.

Thickness (m)	***Re* number**	**Velocity @1170°C for laminar flow (m.s^{-1})**	**Velocity @1170°C for turbulent flow (m.s^{-1})**
20	47000	99	28
15	20000	55	22
10	6000	25	16
5	700	6	9

4.5 Length and Volume

The length of the Pampas Onduladas flow was measured from the far eastern end of La Carbonilla fracture to 35 km north of Puelén (Figure 1) in the province of La Pampa. The length is estimated to be 167 km (following the method by Cashman et al., 2013; see Section 3 Methods). This value is slightly less than previous measurements of 174 km and 181 km (Pasquarè et al., 2005; Pasquarè et al., 2008, respectively). This variation is attributed to the uncertainty in assessing the initial eruption point and the final point of the Pampas Onduladas flow as the eruption point for the Pampas Onduladas flow has not been identified. In this sense Pasquarè et al. (2005 and 2008) provided some general description of the initial and terminal point of the flow determining that its proximal part belongs to the eastern end of the Payún fissure system (also referred to as La Carbonilla fracture) while the end point was located in the Salado river valley in the province of La Pampa (Pasquarè et al., 2008). The length of La Carbonilla fracture on its eastern side is ~ 14 km (Llambías et al., 2010) therefore, providing a wide area from which the Pampas Onduladas eruption point might be.

The flow volume was calculated to be 7.2 km^3, while the surface area was calculated as 739 km^2 (Table 4). The calculated volume should be regarded as a minimum as the base of the flow was extrapolated from the adjacent topography, which may not represent its true basal surface. The topographic slope from the initial to the final part of the flow is 0.84% or 0.24°; however, the slope is not constant along the length. The slope is much steeper in the initial part than in most of its length (Figure 8) as it changes from 1.6% in section 1, to 0.9% in section 2 and then to 0.6, 0.5 and 0.4% in sections 3, 4, and 5, respectively. The mean width of the flow decreases downhill from 9.4 km in section 1, to 5.1 km in section 2, then to 3.8, 2.6 and 3.5 km in sections 3, 4 and 5, respectively.

Table 4: Area and volume calculated for the 5 sections of the Pampas Onduladas flow, as well as for the volcanic cones and the void areas that interrupted the flow.

Sector	**Area (km^2)**	**Volume (km^3)**
1	303	3.9
2	166	1.3
3	100	1.1
4	81	0.8
5	102	0.3
volcanic cones	4	0.1
voids	8	0.1
total for flow	739	7.2

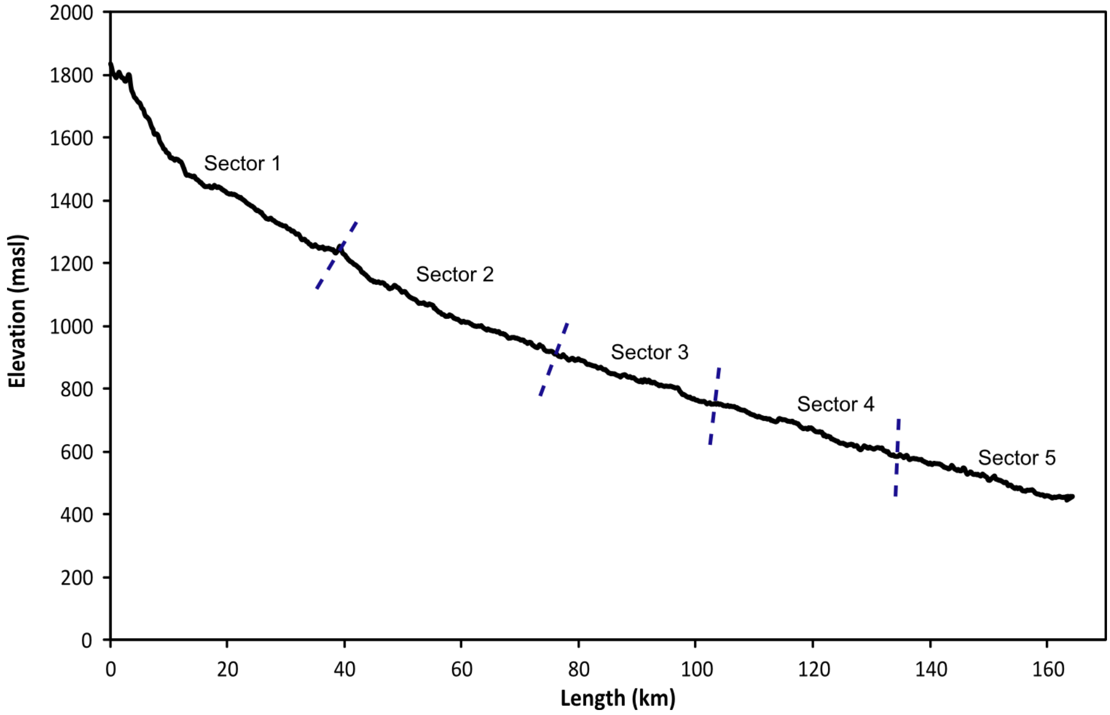

Figure 8: Elevation profile of the Pampas Onduladas flow from its initial (proximal) part to its final (distal) part. Dashed lines separate the five sectors into which the Pampas Onduladas flow was divided.

5 Discussion

5.1 Geochonology

The $^{40}Ar/^{39}Ar$ dating results for the Pampas Onduladas flow, provide the first direct radiometric age for this long flow. The highly precise plateau age of 373 ± 10 ka (3%; 2σ) determined for sample VRE20 is considered to represent the eruption age of the basalt, supported by inverse isochron analysis. The argon isotopic ratios measured for VRE46a appear disturbed, and the decrease in apparent age with increasing temperature is attributed to significant recoil loss/redistribution in this sample. This is consistent with petrographic studies revealing minor alteration (Figure 4f and h) mainly of the interstitial microcrystalline to cryptocrystalline material in this sample. Therefore determination of an eruption age is not possible for this sample, as total gas ages for samples affected by recoil only can be good approximations for eruption age (although these are not so reliable as we cannot be sure that the trapped component is atmospheric, therefore they may overestimate the eruption age), as looks to be the case in this instance, due to consistency with VRE20 results. An eruption age of 373 ± 10 ka (3%; 2s) determined from the Pampas Onduladas flow is stratigraphically consistent with a K-Ar age of 400 ± 100 ka (2σ) previously reported for an underlying basalt flow (see section 2.2).

5.2 Petrogenesis of the Pampas Onduladas Flow

The origin of magma for the Pampas Onduladas flow has been regarded previously as having been affected by metasomatism of the subducting slab (Pasquarè et al., 2008). Trace-element compositions lack typical arc-related signatures such as negative Nb, Ta and Ti anomalies, high Ba/Ta and La/Ta, and enrichment in Th (inferred from slab sediments and slab partial melts, Jacques et al., 2013) or strong depletion in heavy rare earth elements (relative to slab partial melts; Figure 3 b, e). Therefore, the geochemical data suggest that the Pampas Onduladas flow does not exhibit signatures typical of the Andean arc (Figure 7).

The volcanism in the Payún Matrú Volcanic Field (PMVF) is intraplate with a geochemical composition similar to that of ocean island basalts (Germa et al., 2010, Jacques et al., 2013; Søager et al., 2013; Espanon et al., 2014). The composition of the Pampas Onduladas flow also suggests some association with a local intraplate source (Figure 7b; local intraplate source is here taken as the Rio Colorado field). The trace-element ratios show values intermediate to those of the local intraplate (Rio Colorado field, Figure 7) and the lower continental crust (LCC) (Figure 7b, c, d). They also define a linear trend following the local intraplate-LCC regression line (Figure 7c and d), suggesting that some lower crustal assimilation has taken place. Typical LCC signatures include depletion in Th, K, Rb, Zr, Ba, LREE, Hf, and U relative to the local intraplate, slab components (sediments and partial melts) and Andean arc. The samples from the Pampas Onduladas flow show depletion in all of these elements and have high Th/U ratios (LCC = 6). Furthermore, Pasquarè et al. (2008) proposed sialic crustal assimilation for the Pampas Onduladas flow, based on Sr isotopic analyses. The issue of crustal contamination in the PMVF is not clear as there are no crustal Sr-isotopic values for this area (Espanon et al., 2014). The Sr isotope values for the Pampas Onduladas flow are in agreement with those previously presented for the PMVF (Pasquarè et al., 2008; Bertotto et al., 2009; Hernando et al., 2012; Jacques et al., 2013; Søager et al., 2013; Espanon et al., 2014).

As discussed above, geochemical data for the Pampas Onduladas flow are consistent with an intraplate volcanic signature of OIB affinity. It is noted that an intraplate signature is typical of other long (>100 km) basaltic flows such as the Toomba and Undara flows that are associated with mantle upwelling (Stephenson et al., 1998). This is intuitively predictable, as a magmatic body rising from the mantle, would be possessed of the high temperatures, low viscosity and high lava volumes expected to yield long lava flows. However, these magmatic characteristics are common to many volcanic settings, and yet long flows (>100 km) are not common. Rheological and topographical factors that may permit emplacement of a long flow are discussed in the following section

5.3 Rheology of the Pampas Onduladas flow

Formerly, it was generally accepted that long flows (>100 km, Keszthelyi and Self, 1998) require low viscosity, rapid emplacement (Walker, 1973) and large volumes (Pinkerton and Wilson, 1994). However, it has been proposed that effective insulation, in combination with a favourable topographic slope, can also contribute to form long basaltic flows (Keszthelyi and Self, 1998). Based on rheological characteristics, Keszthelyi and Self, (1998), modelled two types of emplacement for long lava flows (>100km); “rapid” and “insulated” models. “Rapid” emplacement requires less than 0.5°C/km of cooling at high velocities of 2 - 15 $m.s^{-1}$ for a channel 2 - 19 m deep and high effusion rates 200 – 17000 m^3/s (Keszthelyi and Self, 1998). On the contrary, “insulated” emplacement requires much lower velocities (0.1 - 1.4 $m.s^{-1}$), slightly thicker flows 2 - 23 m and lower effusion rates 8 – 7100 m^3/s (Keszthelyi and Self, 1998). The calculated viscosity for the Pampas Onduladas flow is in agreement with previous viscosity calculations for long basaltic flows (Stephenson et al., 1998; Pasquarè et al., 2008). The viscosity of a flow increases with concentrations of solids, water and dissolved gases. Pinkerton and Stevenson (1992) suggested that for solid concentrations below 30%, the viscosity remains relatively constant and flow behaviour is approximately that of a Newtonian fluid. In the case of the Pampas Onduladas flow, the viscosity was calculated based on a 15% solid concentration, while Pasquarè et al. (2008) assumed a phenocryst-free magma in their calculation. In both cases the calculated average viscosity is similar (2- 73 Pa.s Pasquarè et al., 2008 and 96 Pa.s current study); therefore, provided the concentration of solids is less than 30%, viscosity values remain low. Nevertheless, the vesicle volume proportion affects the average viscosity of the Pampas Onduladas flow as it increases by from 20 to 30%. Nevertheless, in agreement with the internal morphology of a basaltic flow, the vesicles can be associated with a viscosity reduction, as the pressure imposed by spherical bubbles is not absorbed by the system, but released as the vesicles deform and collapse (Llambías 2008). In Section 2.2, the internal structure of the Pampas Onduladas flow is described as having disrupted and elongated vesicles forming the lower massive layer, agreeing with the previous statement. Despite, the possibility of keeping the flow at low viscosity by vesicle deformation and collapse as previously mentioned, the sub-angular vesicle in Figure 4f and h suggest a transition to a more viscous character in the distal part. This constitutes the only evidence of a change in flow regime; therefore further studies along the flow are needed in order to fully assess the hypothesis of a viscosity change.

The calculated velocity for the Pampas Onduladas flow (Table 3) is higher than previous open channel basaltic flow velocity estimates (4-12 $m.s^{-1}$, Keszthelyi and Self, 1998). The high velocities determined here are regarded as maxima, as the velocity is dependent on thickness, slope and viscosity. The thickness of the flow is one of the largest sources of error. This is because inflation can take place after emplacement and cooling, hence resulting in an apparent thicker flow. In Hawaii, Hon et al. (1994) observed that a flow initially 30 cm thick was inflated to a thickness of 3-7 m in a period of over a week. In the current study several thicknesses (20, 15, 10 and 5 m) were considered in order to estimate the flow velocity, showing that it becomes turbulent at thicknesses greater than 5 m (Table 3). The velocity calculated for a 5 m thick flow (6 $m.s^{-1}$, Table 3) can be regarded as an appropriate value, as it is within the range of open-channel basaltic flows (see Keszthelyi and Self, 1998). Velocities calculated here are higher than the estimate of 1.4 $m.s^{-1}$ from Keszthelyi and Self (1998) for a sheet flow with a slope of 0.1%, an upper lava crust 1 m thick and a total thickness of 23 m. Furthermore, the same authors proposed that faster flows (>5 $m.s^{-1}$) would tend to have a thinner upper crust (<1 m thick), which agrees with the average <1 m thin Pampas Onduladas crust (Pasquarè et al., 2008).

In relation to other long basaltic flows on Earth, the calculated volume for the Pampas Onduladas flow is 7.2 km^3, which is lower than the volume calculated for the Toomba (12 km^3) and for the Undara flow (approximately 25 km^3; Stephenson et al., 1998). Furthermore, in their model Keszthelyi and Self, (1998) proposed that the minimum volume for a 10 m thick long flow (>100 km in length) is 10 km^3. The calculated volume is much lower than previous calculated volumes for long flows on Earth, mostly resulting from the flat pre-flow topography assumption, therefore regarded as minimum.

5.4 Aspects of Pampas Onduladas pre-flow topography

The average slope of the Pampas Onduladas flow (0.84%) is greater than the slope of the Toomba, Undara and Thjotsa flows (0.4%, 0.5% and ~0.7% respectively, Keszthelyi and Self, 1998). Other Quaternary flows in the Pampas Onduladas region have been emplaced over an Andean piedmont topography that created a gradual and lengthy declining slope towards the east. The pre-existing topography is covered mainly by basaltic flows with some exposures of the uplifted San Rafael Block (SRB), characterised by Permian-Triassic volcanic and plutonic assemblages (Figure 1b and Figure 5a, b). The SRB acted as a wall on the northern part of sector 1 and 2, as is evident in cross section A-A’ and B-B’ (Figure 5). The eruption point for this flow has been associated with the activity in La Carbonilla Fracture (LCF in Figure 1; Pasquarè et al. 2008). Here, the topography is characterised by a high elevation resulting from uplift of the Payún Matrú eastern shield when it was magmatically active.

The Pampas Onduladas basalt flowed from its initial point over an irregular topography following its steepest course down-slope. The high slope suggests that the flow followed an unencumbered path, inferred from the long profile (Figure 8), while the irregular topography can be partly inferred from the cross sections. Accordingly, the Pampas Onduladas flow has a positive relief in relation to the surrounding topography in the middle and distal sectors (Figure 5 cross sections C-C', D-D' and E-E'). Interestingly, the cross-section from sector 1, shows a rough surface corresponding to the flow, which has been confined on its northern side by the San Rafael Block and by a topographic high on its southern part (Figure 5, cross section A-A'). Furthermore, in the cross-section from sector 2 (Figure 5, cross-section B-B') the topography adjacent to the flow shows higher elevation, suggesting that the flow has followed a pre-existing topographic depression at least in some areas. This observation is critical in the volume calculation which can lead to underestimation assuming a flat base. Furthermore by following a topographic depression, the flow is insulated possibly resembling the type of effective insulation observed in lava tubes. The Pampas Onduladas has inflation structures such as tumuli and lava rises which are generally associated with pahoehoe sheet flow. No lava tubes have been identified for this basaltic flow. However, it is likely that at least in the proximal part, the flow was confined enhancing the insulation process.

The geochemical, rheological and topographical constraints presented here suggest that the Pampas Onduladas flow shows a combination of characteristics that assisted in the development of its great length. The extent of the Pampas Onduladas flow cannot be explained by its geochemical characteristics as it shares these with other basalts of the PMVF. Thus, it is likely that its exceptional length is related to a steep slope, aided by low viscosity and a good insulating system derived from its inflating nature and topographic confinement.

6 Conclusions

The Pampas Onduladas flow in southern Mendoza constitutes one of the four longest Quaternary lava flows on Earth. It was erupted during the pre-caldera basaltic volcanism of the Payún Matrú volcanic field (Hernando et al., 2012) as confirmed by the geochronological data. The $^{40}Ar/^{39}Ar$ analysis suggests an eruption age of 373 ± 10 ka (2σ), constituting the first direct age constraint for this flow. Geochemical characteristics are consistent with an intraplate setting. This corresponds to a negligible arc signature, an enriched mantle source similar to local ocean island basalts (Rio Colorado volcanic field; Søager et al., 2013) and possible lower continental crust assimilation (Germa et al., 2010; Jacques et al., 2013; Søager et al., 2013; Espanon et al., 2014)

Rheological characteristics indicate that the viscosity was low and the average eruption temperature was 1170°C. An important feature is the topographic slope which is higher (0.84%) than that determined for the Undara (0.5%), Toomba (0.4%) (Stephenson et al.,

1998) and Thjorsa (~0.7) (Vilmundardottir, 1977) flows. The slope is likely to be the most important feature affecting the length (Keszthelyi and Self, 1998) and velocity. The calculated velocity varies depending on thickness, from 30 $m.s^{-1}$ (>110 $km.h^{-1}$) to 17 $m.s^{-1}$ (~60 $km.h^{-1}$) for 20 m and 10 m thickness, respectively (turbulent velocities for flow thickness values >5 m). The proposed thickness is at least 20 m (Pasquarè et al., 2008), after the flow inflated and cooled. The original thickness however, could have been ten times smaller than that preserved, using the inflation ratios from Hon et al. (1994) for Hawaiian basalts. The volume calculated here (7.2 km^3) is regarded as a minimum estimate, based on the method used, which assumes a flat surface below the flow. The length of the Pampas Onduladas flow is not governed by its geochemical characteristics, but by the steep and constant topographic slope supported by an effective insulating system and low viscosity.

Acknowledgments

We greatly thank the park rangers at Llancanelo and Payunia Provincial Natural Reserve (Mendoza), Stephanie Kerr, Paul Connolly and Adriana Garcia for their help and assistance during field trips, Jan-Hendrik May for his assistance with spatial analysis and Stan Szczepanski for technical support with $^{40}Ar/^{39}Ar$ analysis. We acknowledge the Renewable Natural Resources division of the Province of Mendoza for providing access permits. We are grateful to Dr Karoly Nemeth and anonymous reviewer for their comments which considerably improved the manuscript. AD acknowledges Australian Research Council Future Fellowship FT0990447.

Appendix A (equations used for turbulent flow calculations)

1- Reynolds number (*Re*)

$$Re = \frac{\rho H v}{\eta}$$

Where ρ is density, H is the thickness, v is the velocity and η is the viscosity

2- Chezy equation

$$v^2 = \frac{g H \theta}{C_f}$$

Where v is the velocity for a turbulent flow, g is the gravitational acceleration, H is the thickness, θ is the slope and C_f is the friction coefficient

3- Goncharov equation (Goncharov, 1964) to determine the friction coefficient for a turbulent flow with *Re* < 10^5

$$C_f = \frac{\lambda}{2}$$

$$\lambda = \{4 \log_{10}[6.15((Re' + 800)/41)^{0.92}]\}^{-2}$$

$$Re' = 2Re$$

References

Bermúdez, A., Delpino, D. 1989. La Provincia Basaltica Andino Cuyana (35-37°L.S.). Revista de la Asociación Geológica Argentina, 44 (1-4): 35-55.

Bertotto, G., Cingolani, C., Bjerg, E. 2009. Geochemical variations in Cenozoic back-arc basalts at the border of La Pampa and Mendoza provinces, Argentina. Journal of South American Earth Sciences, 28 (4): 360-373. DOI:10.1016/j.jsames.2009.04.008

Bottinga, Y. A., Weil, D. F. 1972. The viscosity of magmatic silicate liquids: a model for calculation. American Journal of Science, 272 (5): 438-473. DOI: 10.2475/ajs.272.5.438

Cassata, W. S., Singer, B. S., Cassidy, J. 2008. Laschamp and Mono Lake geomagnetic excursions recorded in New Zealand. Earth and Planetary Science Letters, 268 (1): 76-88. DOI: 10.1016/j.epsl.2008.01.009

Cashman, K., Soule, S., Mackey, B., Deligne, N., Deardorff, N., Dietterich, H. 2013. How lava flows: New insights from applications of lidar technologies to lava flow studies. Geosphere, 9 (6): 1664-1680. DOI: 10.1130/GES00706.1

Costa, F. G., Singer, B. S. 2002. Evolution of Holocene dacite and compositionally zoned magma, volcán San Pedro, Southern Volcanic Zone, Chile. Journal of Petrology, 43 (8): 1571-1593. DOI: 10.1093/petrology/43.8.1571

Espanon, V. R., Chivas, A. R., Kinsley, L. K. J., Dosseto, A., 2014. Geochemical variations in the Quaternary Andean back-arc volcanism, southern Mendoza, Argentina. Lithos, 208-209: 251-264. DOI: 10.1016/j.lithos.2014.09.010

Ferguson, K. M., Dungan, M. A., Davidson, J. P., Colucci, M. T. 1992. The Tatara-San Pedro volcano, 36°S, Chile: A chemically variable, dominantly mafic magmatic system. Journal of Petrology, 33 (1): 1-43. DOI: 10.1093/petrology/33.1.1

Germa, A., Quidelleur, X., Gillot, P. Y., Tchilinguirian, P. 2010. Volcanic evolution of the back-arc Pleistocene Payun Matru volcanic field (Argentina). Journal of South American Earth Sciences, 29: 717-730. DOI: 10.1016/j.jsames.2010.01.002

Goncharov, V. 1964. Dynamics of Channel Flow, 317 pp., translated from Russian by Israel Program Sci. Transl., US Dep. of Commer., Off. of Tech. Serv., Washington, DC.

Gudnason, J., Holm, P. M., Søager, N., Llambias, E. J. 2012. Geochronology of the late Pliocene to Recent volcanic activity in the Payenia back-arc volcanic province, Mendoza, Argentina. Journal of South American Earth Sciences, 37: 191-201. DOI: 10.1016/j.jsames.2012.02.003

Halldorsson, S. A., Oskarsson, N., Gronvold, K., Sigurdsson, G., Sverrisdottir, G., Steinthorsson, S. 2008. Isotopic-heterogeneity of the Thjorsa lava-implications for mantle sources and crustal processes within the Eastern Rift Zone, Iceland. Chemical Geology, 255 (3): 305-316. DOI: 10.1016/j.chemgeo.2008.06.050

Hernando, I. R., Llambías, E. J., González, P. D., Sato, K. 2012. Volcanic stratigraphy and evidence of magma mixing in the Quaternary Payun Matru volcano, Andean backarc in western Argentina. Andean Geology, 39 (1): 158-179.

Hernando, I. R., Franzese, J. R., Llambías, E. J., Petrinovic, I. A. 2014. Vent distribution in the Quaternary Payún Matrú Volcanic Field, western Argentina: Its relation to tectonics and crustal structures. Tectonophysics, 622: 122-134. DOI: 10.1016/j.tecto.2014.03.003

Hon, K., Kauahikaua, J., Denlinger, R., Mackay, K. 1994. Emplacement and inflation of pahoehoe sheet flows: Observations and measurements of active lava flows on Kilauea Volcano, Hawaii. Geological Society of America Bulletin, 106 (1): 351-370. DOI: 10.1130/0016-7606

Inbar, M., Risso, C. 2001. A morphological and morphometric analysis of a high density cinder cone volcanic field - Payun Matru, south-central Andes, Argentina. Zeitschrift für Geomorphologie, 45 (3): 321-343.

Jacques, G., Hoernle, K., Gill, J., Hauff, F., Wehrmann, H., Garbe-Schönberg, D., Van Den Bogaard, P., Bindeman, I., Lara, L. E. 2013. Across-arc geochemical variations in the Southern Volcanic Zone, Chile (34.5-38.0°S): Constraints on mantle wedge and slab input compositions. Geochimica et Cosmochimica Acta, 123: 218 - 243.

DOI: 10.1016/j.gca.2013.05.016

Jeffreys, H ., 1925. The flow of water in an inclined channel of rectangular section. Philosophical Magazine, 49 (293), 793-807. DOI:10.1080/14786442508634662

Kay, S. M., Gorring, M., Ramos, V. A. 2004. Magmatic sources, setting and causes of Eocene to Recent Patagonian plateau magmatism (36°S to 52°S latitude). Revista de la Asociación Geológica Argentina, 59 (4): 556-568.

Kay, S. M., Burns, W. M., Copeland, P., Mancilla, O. 2006. Upper Cretaceous to Holocene magmatism and evidence for transient Miocene shallowing of the Andean subduction zone under the northern Neuquén basin. Geological Society of America Special Paper, 407, 19-60. DOI: 10.1130/2006.2407(02)

Kay, S. M., Jones, H. A., Kay, R. W., 2013. Origin of Tertiary to Recent EM-and subduction-like chemical and isotopic signatures in Auca Mahuida region (37°–38° S) and other Patagonian plateau lavas. Contributions to Mineralogy and Petrology, 166 (1): 165-192. DOI: 10.1007/s00410-013-0870-9

Keszthelyi, L., Pieri, D. C., 1993. Emplacement of the 75-km-long Carrizozo lava flow field, south-central New Mexico. Journal of Volcanology and Geothermal Research, 59 (1-2): 59-75. DOI: 10.1016/0377-0273(93)90078-6

Keszthelyi, L., Self, S. 1998. Some physical requirements for the emplacement of long basaltic lava flows. Journal of Geophysical Research, 103 (B11): 27447 - 27464.

Keszthelyi, L., Thordarson, T., Mcewen, A., Haack, H., Guilbaud, M. N., Self, S., Rossi, M. J. 2004. Icelandic analogs to Martian flood lavas. Geochemistry, Geophysics, Geosystems, 5 (11). DOI: 10.1029/2004GC000758

Koppers, A. A. P., Staudigel, H., Wijbrans, J. R. 2000. Dating crystalline groundmass separates of altered Cretaceous seamount basalts by the $^{40}Ar/^{39}Ar$ incremental heating technique. Chemical Geology, 166 (1-2): 139-158. DOI: 10.1016/S0009-2541(99)00188-6

Llambías, E. J. 2008. Geología de los cuerpos ígneos, Buenos Aires, Argentina. Asociación Geológica Argentina.

Llambías, E. J., Bertotto, G., Risso, C. & Hernando, I. 2010. El volcanismo Cuaternario en el retroarco de Payenia: Una revision. Revista de la Asociación Geológica Argentina, 67 (2): 278-300.

Lipman, P. W., Banks, N. G., 1987. Aa Flow Dynamics, Mauna Loa 1984, U.S. Geological Survey Professional Paper, vol. 1350: 1527-1567.

Lopez-Escobar, L., Frey, F. A., Vergara M. M., 1977. Andesites and high-alumina basalts from the central-south Chile high Andes: geochemical evidence bearing on their petrogenesis. Contributions to Mineralogy and Petrology, 63 (3): 199-228. DOI: 10.1007/BF00375573

Ludwig, K. R. 2012. User's Manual for Isoplot 3.75. A geochronological toolkit for Microsoft Excel. Special Publication No. 5. Berkeley Geochronology Center, Berkeley, California, p. 75.

Matchan, E. L., Phillips, D., 2014. High precision multi-collector $^{40}Ar/^{39}Ar$ dating of young basalts: Mount Rouse volcano (SE Australia) revisited. Quaternary Geochronology 22: 57-64. DOI: 10.1016/j.quageo.2014.02.005

McDonough, W. F., Sun, S.-S. 1995. The composition of the Earth. Chemical Geology, 120 (3-4): 223-253. DOI: 10.1016/0009-2541(94)00140-4

Melchor, R., Casadío, S. 1999. Hoja Geológica 3766-III La Reforma, provincia de La Pampa. Secretaría de Minería de la Nación, Servicio Geológico Argentino. Boletín 295, Buenos Aires.

Méndez, V., Zanettini, J. C., Zappettini, E. O. 1995. Geología y metalogénesis del Orógeno andino central, República Argentina, Secretaría de Minería de la Nación, Dirección Nacional del Servicio Geológico.

Narciso, V., Santamaría, G., Zanettini, J. 2001. Hoja Geológica 3769-1, Barrancas. Provincias de Mendoza y Neuquén. Instituto de Geología y Recursos Minerales, Servicio Geológico Minero Argentino, Boletín, 253.

Nemeth, K., Haller, M., Martin, C., Risso, C., Massaferro, G. 2008. Morphology of lava tumuli from Mendoza (Argentina), Patagonia (Argentina), and Al-Haruj (Libya). Zeitschrift für Geomorphologie, 52 (2): 181-194.

Nier, A. O., 1950. A redetermination of the relative abundances of the isotopes of carbon, nitrogen, oxygen, argon, and potassium. Physical Review 77: 789-793. DOI: http://dx.doi.org/10.1103/PhysRev.77.789

Núñez, E., 1976. Descripción geológica de la Hoja 31e Chical-Có, provincias de Mendoza y La Pampa. Servicio Nacional Geológico Minero, Informe Inédito. Buenos Aires.

Pasquarè, G., Bistacchi, A., Mottana, A. 2005. Gigantic individual lava flows in the Andean foothills near Malargue (Mendoza, Argentina). Rendiconti Lincei. Scienze Fisiche e Naturali, 16: 127-135.

Pasquarè, G., Bistacchi, A., Francalanci, L., Bertotto, G., Boari, E., Massironi, M., Rossotti, A. 2008. Very long pahoehoe inflated basaltic lava flows in the Payenia Volcanic Province (Mendoza and La Pampa, Argentina). Revista de la Asociación Geológica Argentina, 63 (1): 131-149.

Phillips, D., Matchan, E. L. 2013. Ultra-high precision $^{40}Ar/^{39}Ar$ ages for Fish Canyon Tuff and Alder Creek Rhyolite sanidine: New dating standards required? Geochimica et Cosmochimica Acta, 121: 229-239. DOI: 10.1016/j.gca.2013.07.003

Pinkerton, H., Stevenson, R. 1992. Methods of determining the rheological properties of lavas from their physico-chemical properties. Journal of Volcanology and Geothermal Research, 53 (1-4): 47-66. DOI: 10.1016/0377-0273(92)90073-M

Pinkerton, H., Wilson, L. 1994. Factors controlling the lengths of channel-fed lava flows. Bulletin of Volcanology, 56 (2): 108-120. DOI: 10.1007/BF00304106

Polanski, J. 1954. Rasgos geomorfológicos del territorio de la provincia de Mendoza. Instituto de Investigaciones Económicas y Tecnológicas, Cuadernos de Estudio e Investigación. Mendoza.

Ramos, V. A., Folguera, A. 2011. Payenia volcanic province in the Southern Andes: An appraisal of an exceptional Quaternary tectonic setting. Journal of Volcanology and Geothermal Research, 201 (1-4): 53-64. DOI: 10.1016/j.jvolgeores.2010.09.008

Reynolds, A. J. 1974. Turbulent Flow in Engineering, New York, John Wiley.

Rivalenti, G., Mazzucchelli, M., Laurora, A., Ciuffi, S. I. A., Zanetti, A., Vannucci, R., Cingolani, C. 2004. The backarc mantle lithosphere in Patagonia, South America. Journal of South American Earth Sciences, 17 (2): 121–152. DOI: 10.1016/j.jsames.2004.05.009

Rodriguez, E., Morris, C. S., Belz, J. E. 2006. A global assessment of the SRTM performance. Photogrammetric Engineering and Remote Sensing, 72 (3): 249-260. DOI: 10.14358/PERS.72.3.249

Rudnick, R. L., Gao, S. 2003. Composition of the Continental Crust. In: Holland, H.D., Turekian, K.K., (Eds), Treatise on Geochemistry 3: The Crust, 1-64. DOI: 10.1016/B0-08-043751-6/03016-4

Singer, B.S., Pringle, M.S. 1996. Age and duration of the Matuyama-Brunhes geomagnetic polarity reversal from $^{40}Ar/^{39}Ar$ incremental heating analyses of lavas. Earth and Planetary Science Letters, 139 (1-2): 47-61. DOI: 10.1016/0012-821X(96)00003-9

Sisson, T. W., Grove, T. L. 1993. Experimental investigations of the role of H_2O in calc-alkaline differentiation and subduction zone magmatism. Contributions to Mineralogy and Petrology, 113 (2): 143-166. DOI: 10.1007/BF00283225

Smith, M. J., Rose, J., Gousie, M. B. 2009. The Cookie Cutter: A method for obtaining a quantitative 3D description of glacial bedforms. Geomorphology, 108 (3-4): 209-218. DOI: 10.1016/j.geomorph.2009.01.006

Søager, N., Holm, P. M., Llambías E. J. 2013. Payenia volcanic province, southern Mendoza, Argentina: OIB mantle upwelling in a backarc environment. Chemical Geology, 349-350: 36-53. DOI: 10.1016/j.chemgeo.2013.04.007

Steiger, R. H., Jäger, E., 1977. Subcommission on geochronology: convention on the use of decay constants in geo-and cosmochronology. Earth and Planetary Science Letters, 36 (3): 359-362. DOI: 10.1016/0012-821X(77)90060-7

Stephenson, P. J., Burch-Johnston, A. T., Stanton, D., Whitehead, P. W. 1998. Three long lava flows in north Queensland. Journal of Geophysical Research, 103 (B11): 27359-27370.

Stern, C. R., Frey, F. A., Futa, K., Zartman, R. E., Peng, Z., Kyser, T. K. 1990. Trace-elements and Sr, Nd, Pb and O isotopic composition of Pliocene and Quaternary alkali basalts of the Patagonian Plateau lavas of southernmost South America. Contributions to Mineralogy and Petrology, 104 (3): 294-308. DOI: 10.1007/BF00321486

Stern, C. R. 2004. Active Andean volcanism: its geologic and tectonic setting. Revista Geológica de Chile, 31 (2): 161-206.

Tazieff, H. 1977. An exceptional eruption: Mt. Niragongo, Jan. 10^{th}, 1977. Bulletin of Volcanology, 40 (3): 189-200. DOI: 10.1007/BF02596999

Thorpe, R. S. 1984. The tectonic setting of active Andean volcanism. In Andean magmatism: Chemical and Isotopic Constraints. Shiva Geological Series, Shiva Publications, Nantwich, U.K., p. 4-8.

Tormey, D. R., Hickey-Vargas, R., Frey, F. A., Lopez-Escobar, L. 1991. Recent lavas from the Andean volcanic front (33 to 42°S); interpretations of along-arc compositional variations. Special Paper Geological Society of America, 265: 57-78. DOI: 10.1130/SPE265-p57

Tormey, D. R., Frey, F. A., Lopez-Escobar, L. 1995. Geochemistry of the active Azufre-Planchon-Peteroa Volcanic Complex, Chile (35°15'S): Evidence for multiple sources and processes in a cordilleran arc magmatic system. Journal of Petrology, 36 (2): 265-298. DOI: 10.1093/petrology/36.2.265

Turrin, B. D., Donnelly-Nolan, J. M., Hearn Jr., B. C., 1994. $^{40}Ar/^{39}Ar$ ages from the rhyolite of Alder Creek, California: age of the Cobb mountain normal-polarity subchron revisited. Geology 22 (3): 251-254. DOI: 10.1130/0091-7613(1994) 22<0251:AAAFTR>2.3.CO;2

Vilmundardottir, E. G., 1977. Tungnarhraun, Orustofnun geologic report, Rep. OS ROD 7702, 156 pp., Reykjavik.

Walker, G. P. 1973. Length of lava flows. Philosophical Transactions of the Royal Society A 274 (1238): 107-118. DOI: 10.1098/rsta.1973.0030

Williams, H., McBirney, A. 1979. *Volcanology,* San Francisco, Freeman, Cooper and Company.